

# Microwave dielectric properties of SnO-SnF<sub>2</sub>-P<sub>2</sub>O<sub>5</sub> glass and its composite with alumina for ULTCC applications

Indira J. Induja<sup>1</sup> | Mailadil T. Sebastian<sup>2</sup>

<sup>1</sup>Materials Science & Technology Division, National Institute for Interdisciplinary Science Technology, Thiruvananthapuram, India

<sup>2</sup>Microelectronics Research Unit, Faculty of Information Technology & Electrical Engineering, University of Oulu, Oulu, Finland

## Correspondence

M.T. Sebastian, Microelectronics Research Unit, Faculty of Information Technology & Electrical Engineering, University of Oulu, Oulu, Finland.  
Email: mailadils@yahoo.com

## Abstract

Ultralow-temperature sinterable alumina-45SnF<sub>2</sub>:25SnO:30P<sub>2</sub>O<sub>5</sub> glass (Al<sub>2</sub>O<sub>3</sub>-SSP glass) composite has been developed for microelectronic applications. The 45SnF<sub>2</sub>:25SnO:30P<sub>2</sub>O<sub>5</sub> glass prepared by melt quenching from 450°C has a low  $T_g$  of about 93°C. The SSP glass has  $\epsilon_r$  and  $\tan\delta$  of 20 and 0.007, respectively, at 1 MHz. In the microwave frequency range, it has  $\epsilon_r=16$  and  $Q_u \times f=990$  GHz with  $\tau_f=-290$  ppm/°C at 6.2 GHz with coefficient of thermal expansion (CTE) value of 17.8 ppm/°C. A 30 wt.% Al<sub>2</sub>O<sub>3</sub>-70 wt.% SSP composite was prepared by sintering at different temperatures from 150°C to 400°C. The crystalline phases and dielectric properties vary with sintering temperature. The alumina-SSP composite sintered at 200°C has  $\epsilon_r=5.41$  with a  $\tan\delta$  of 0.01 (1 MHz) and at microwave frequencies it has  $\epsilon_r=5.20$  at 11 GHz with  $Q_u \times f=5500$  GHz with temperature coefficient of resonant frequency ( $\tau_f$ )=-18 ppm/°C. The CTE and room-temperature thermal conductivity of the composite sintered at 200°C are 8.7 ppm/°C and 0.47 W/m/K, respectively. The new composite has a low sintering temperature and is a possible candidate for ultralow-temperature cofired ceramics applications.

## KEYWORDS

composites, dielectric materials/properties, glass-ceramics, LTCC, microwaves

## 1 | INTRODUCTION

There is an increased demand for new materials with attractive dielectric properties in the areas of wireless communication, satellite communication, electronic memory devices, and so on.<sup>1,2</sup> Low-temperature cofired ceramic technology (LTCC) is a well-established multilayer technology having numerous applications.<sup>3</sup> At present, extensive research is being carried out to develop new materials having sintering temperature less than 700°C.<sup>2</sup> Several glass-ceramics, molybdates, vanadates, tungstates, tellurates based ceramics are reported in the literature as ultralow-temperature cofired ceramics (ULTCC) materials.<sup>2</sup> Energy saving, reduction in processing time, as well as cost effectiveness, and cofiring with conductors such as nanosilver ink are the attractive features of ULTCC technology.<sup>2,4</sup> For future applications, there is an urgent demand for the development of new ULTCC materials.<sup>5</sup>

Over the past several years, considerable efforts have been made by researchers to develop new glasses having low glass-transition temperature. Glasses having low glass-transition temperature ( $T_g$ ) offers a wide variety of applications such as glass-metal sealing, IC packaging, and so on.<sup>6</sup> Among them, fluorophosphate glasses are of significant interest. In general fluorophosphate glasses have low  $T_g$  compared to silicate and borate glasses.<sup>7</sup> The optical properties of fluorophosphate glasses are comparable with that of fluoride glasses, and mechanical properties that of oxide glasses.<sup>8</sup> Besides this, another attracting property of phosphate glasses is its ability to associate fluoride compounds without losing the tendency to form glass.<sup>9</sup> Due to the nonlinear refractive index change, fluorophosphate glasses can be qualified as suitable candidates for high-power lasers.<sup>10</sup> Fluorine-containing glasses find application in the field of laser windows, lenses, and filters.<sup>11</sup> The introduction of network modifying cation tin (Sn) lowers the  $T_g$  of fluorophosphate glasses.<sup>12</sup>

Alumina ( $\text{Al}_2\text{O}_3$ ) is considered as the gemstone of the electronic industry due to its excellent electrical and physical properties compared to other ceramics.<sup>13</sup> The sintering temperature of  $\text{Al}_2\text{O}_3$  is relatively high at about 1600°C. The main challenge behind making  $\text{Al}_2\text{O}_3$  as LTCC/ULTCC material is its high sintering temperature.<sup>14,15</sup> Low melting and low-loss glasses are known to be effective sintering aids for reducing the sintering temperature of various ceramics without much affecting the microwave properties.<sup>3</sup> The traditional method to lower the sintering temperature of the  $\text{Al}_2\text{O}_3$  is by glass addition. Several authors reported the effective role of glass in reducing the sintering temperature of  $\text{Al}_2\text{O}_3$ .<sup>16-26</sup>

Several research groups have reported the preparation of ternary glass  $\text{SnO-SnF}_2\text{-P}_2\text{O}_5$ . The structure of SSP glass was studied by spectroscopic methods.<sup>6,27,28</sup> Liu et al. prepared different compositions of SSP glass with  $x\text{SnF}_2\text{-(70-x)SnO-30P}_2\text{O}_5$  glasses ( $x=40, 45, 50, 55, 60$ ), and employed Fourier Transform Infrared and X-ray photoelectron spectroscopy (XPS) techniques to understand the SSP glass structure for the different compositions.<sup>6</sup> From XPS analysis, they found that the change in glass network dimension was responsible for the variation in glass properties for different compositions. They reported that the  $T_g$  value decreases and the coefficient of thermal expansion (CTE) value increases with increase in  $\text{SnF}_2$  content.<sup>6</sup> Although extensive work has been reported on the structure and properties of SSP glass, no attempt was done to study the dielectric properties. In this study, we report the radiofrequency and microwave dielectric properties of SSP glass and its composite with alumina.

## 2 | EXPERIMENTAL PROCEDURE

### 2.1 | Preparation of $45\text{SnF}_2\text{:}25\text{SnO}\text{:}30\text{P}_2\text{O}_5$ glass

Tin-based fluorophosphate ternary glass having the composition  $45\text{SnF}_2\text{:}25\text{SnO}\text{:}30\text{P}_2\text{O}_5$  (SSP) was prepared by conventional melt quenching technique. A two-step melting process was adopted to minimize fluorine loss. Initially ammonium dihydrogen phosphate ( $\text{NH}_4\text{H}_2\text{PO}_4$ ,  $\geq 98\%$ , Sigma Aldrich, St. Louis, MO, USA) was first melted at 450°C for 30 minutes. Then stoichiometrically weighed tin oxide ( $\text{SnO}$ , 99%, Alfa Aesar, Tewksbury, MA, USA) and tin fluoride ( $\text{SnF}_2$ , 99%, Sigma Aldrich) were added one by one to the melt and again heated in the furnace at 450°C for 30 minutes. The whole melt was quenched in distilled water. The molten glass was poured into moulds having different dimensions for dielectric and thermal studies.

### 2.2 | $\text{Al}_2\text{O}_3$ -SSP glass composite preparation

The aim of our work was to develop alumina-SSP glass composite suitable for ULTCC applications. Different weight %

of alumina and SSP glasses had been prepared. Only 30 wt.% alumina and 70 wt.% SSP glass compositions can be sintered below 400°C with good dielectric properties suitable for ULTCC applications. The sintering temperature was found to increase to above the ULTCC range with increase in alumina content. Only the composition which contains 30 wt.%  $\text{Al}_2\text{O}_3$ -70 wt.% SSP glass yields the required ULTCC temperature range. The suitable composition between  $\text{Al}_2\text{O}_3$  and  $45\text{SnF}_2\text{:}25\text{SnO}\text{:}30\text{P}_2\text{O}_5$  glass having low sintering temperature was selected for further studies. The composite with 30 wt.%  $\text{Al}_2\text{O}_3$ -70 wt.%  $\text{SnO-SnF}_2\text{-P}_2\text{O}_5$  glass was prepared by mixing the raw materials using acetone for 10 hours. The slurry was dried and ground well. The  $\text{Al}_2\text{O}_3$ -SSP composite was sintered at different temperatures from 150°C to 400°C.

### 2.3 | Characterization techniques

The amorphous nature of the as-prepared glass as well as the phase composition of the 30 wt.%  $\text{Al}_2\text{O}_3$ -70 wt.%  $\text{SnO-SnF}_2\text{-P}_2\text{O}_5$  glass composite was studied using X-ray diffractometer (XRD) ( $\text{CuK}_\alpha$  radiation, PANalytical X'Pert PRO diffractometer, Netherlands). The spectra of the powder glass were recorded using PerkinElmer Series FT-IR Spectrometer, USA. The glass-transition temperature of the powder glass sample was determined using differential scanning calorimeter (DSC) analysis (TA Instruments Q2000 DSC with Refrigerated Cooling System (RCS), New Castle, DE, USA). For DSC analysis, the glass powder was heated from 30°C to 300°C with a heating rate of 10°/min. Thermo gravimetric/differential thermal analysis (TG/DTA) analysis was done for the glass powder (STA 7300, Thermal Analysis System, Hitachi, Japan) from 30°C to 700°C with a heating rate of 10°/min under nitrogen atmosphere. The density of the SSP glass was measured using Archimedes method using distilled water medium and the density of  $\text{Al}_2\text{O}_3$ -SSP glass composite was determined using dimensional method with the help of a digital screw gauge and weight measured using a semi-micron weighing balance (Shimadzu, AUW220D, Japan). The microstructure of the composite was studied using JOEL-JSM 5600 LV, Tokyo, Japan. The radio (low)-frequency dielectric properties of the glass powder having dimensions 8 mm diameter and 2 mm thickness were determined by parallel plate capacitor method using an inductance capacitance resistance (LCR) meter (Hioki 3532-50LCR Hi Tester, Japan). For the radiofrequency measurements of the bulk  $\text{Al}_2\text{O}_3$ -SSP composite, samples having 11 mm diameter and 1.5 mm thickness, electrode with copper on both sides were used. The thermal conductivity of the composite was measured using a laser flash thermal properties analyzer (Flash-Line2000, Anter Corporation, Pittsburgh, PA, USA). The

thermal expansions of the glass pellet as well as the  $\text{Al}_2\text{O}_3$ -SSP glass composite were measured using thermo mechanical analyzer (Exstar-TMA/SS7300, SII Nano Technology, Inc., Tokyo, Japan). The microwave dielectric properties were measured using a network analyzer (Agilent E5071C ENA series, Agilent Technologies, Santa Clara, CA, USA) operating in the frequency region 300 kHz to 20 GHz. SSP glass samples having 14.2 mm diameter and 6.7 mm thickness were used for microwave

measurements. In the case of  $\text{Al}_2\text{O}_3$ -SSP composites, samples having 11 mm diameter and 5.4 mm thickness were used. The dielectric constant was measured by Hakki-Coleman method.<sup>9</sup> The unloaded quality factor was determined using resonant cavity method in the  $\text{TE}_{018}$  mode.<sup>9</sup> The temperature coefficient of resonant frequency ( $\tau_f$ ) of the SSP glass and the  $\text{Al}_2\text{O}_3$ -SSP glass composite was measured in the temperature range 25°C-60°C using the cavity method.<sup>9</sup>  $\tau_f$  was determined using the formula:

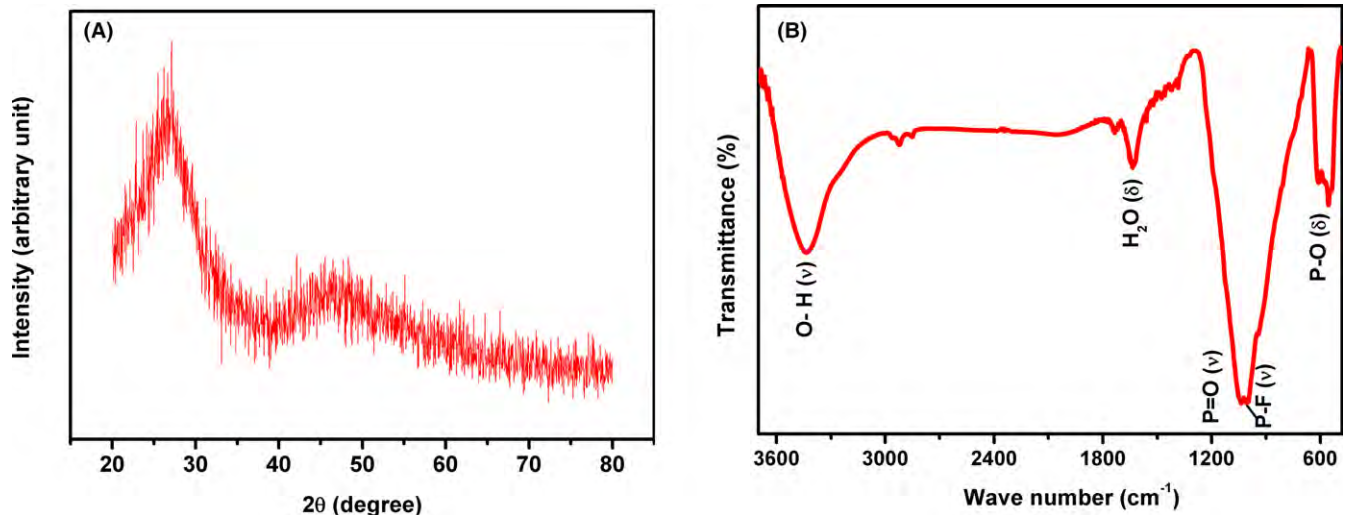


FIGURE 1 XRD pattern (A) and room-temperature FT-IR spectrum (B) of  $45\text{SnF}_2:25\text{SnO}:30\text{P}_2\text{O}_5$  glass

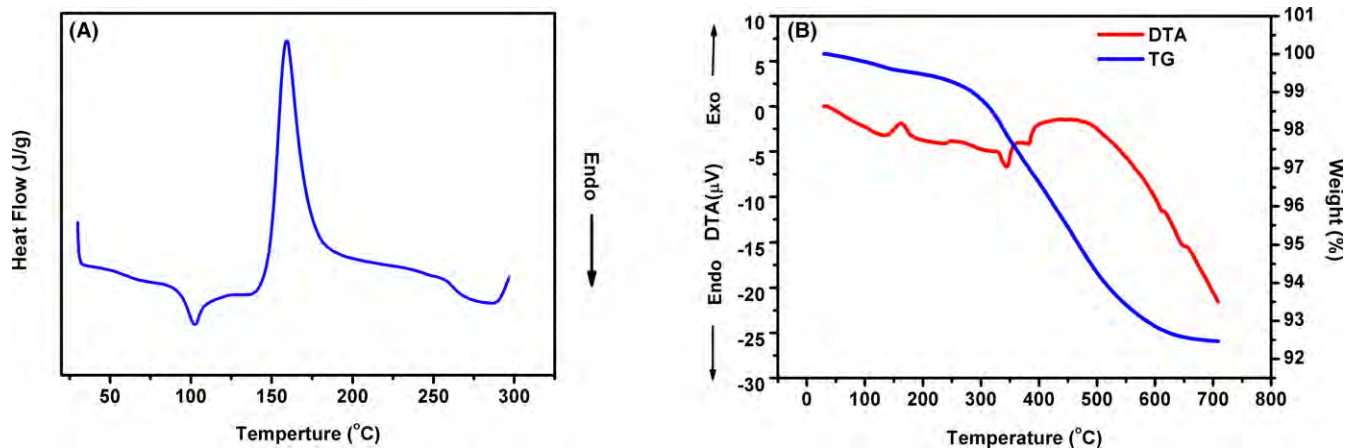


FIGURE 2 DSC and TG/DTA curve of SSP glass powder

TABLE 1 Dielectric properties of SSP glass having density  $4.38 \text{ g cm}^{-3}$

Dielectric properties at 1 MHz		Dielectric properties at 5 GHz using split post dielectric resonator		Dielectric properties at using ;Hakki-Coleman method		
$\epsilon_r$	$\tan\delta$	$\epsilon_r$	$\tan\delta$	$\epsilon_r$ (6.2 GHz) (Hakki)	$Q_u \times f$ (GHz) (Cavity)	$\tau_f$ (ppm/°C)
20	0.02	17	0.006	16	990	-290

SPDR, split post dielectric resonator.

$$f = \frac{1}{f\Delta T} \quad (1)$$

where  $f$  is the resonant frequency at room temperature and  $\Delta f$  is the variation in resonant frequency for a change in  $\Delta T$ .

### 3 | RESULTS AND DISCUSSIONS

#### 3.1 | Structural, dielectric, and thermal properties of SSP glass

Figure 1A shows the XRD pattern of the SSP glass indicating the amorphous nature. The absence of crystalline phase in the XRD confirms the formation of 45SnF<sub>2</sub>:25SnO:

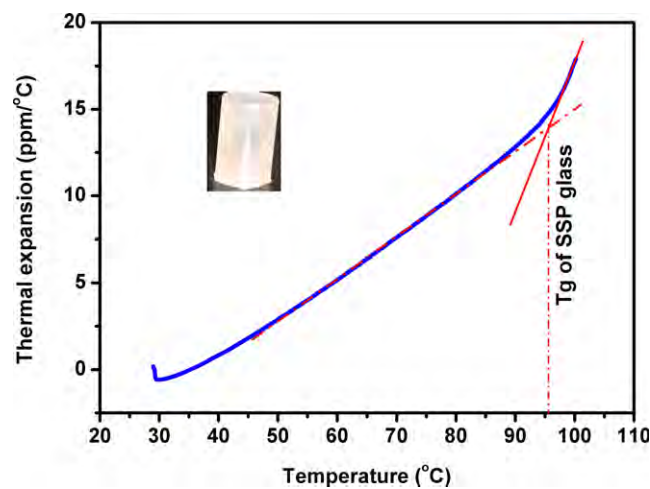
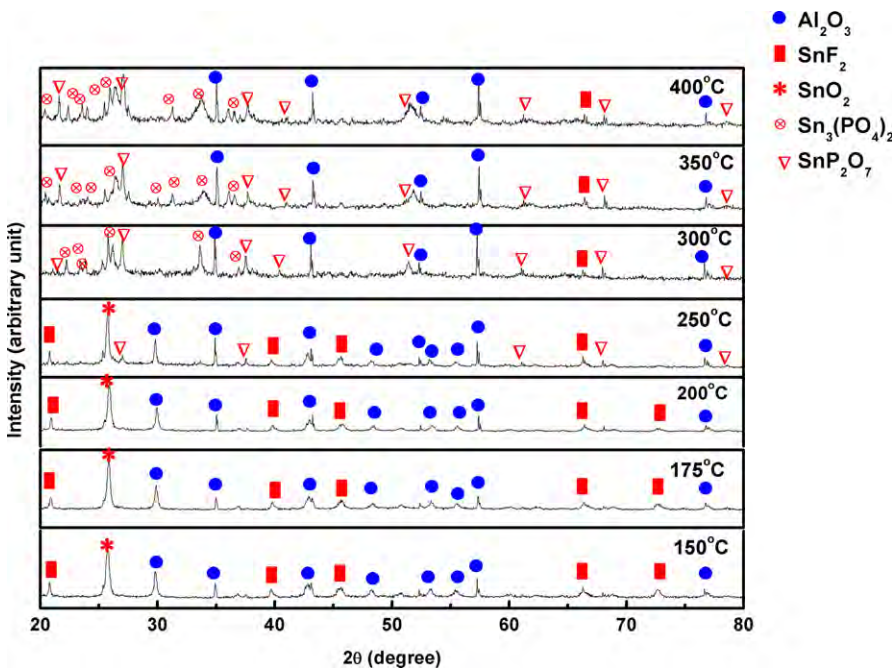


**FIGURE 3** Variation in thermal expansion with temperature for SSP glass

30P<sub>2</sub>O<sub>5</sub> glass prepared by quenching method. Figure 1B shows the room-temperature FT-IR spectrum of 45SnF<sub>2</sub>:25SnO:30P<sub>2</sub>O<sub>5</sub> glass powder in the range 4000 to 400 cm<sup>-1</sup>. The spectra indicate the presence of OH which might be due to the moisture absorption during the preparation of the sample using KBr. The band at 3438 cm<sup>-1</sup> can be attributed to the stretching vibration of O–H bond, 1630 cm<sup>-1</sup> due to the bending vibration of H–OH bond. The bands corresponding to 1100 to 930 cm<sup>-1</sup> is due to the stretching vibration of P=O bond. The band around 630 cm<sup>-1</sup> is attributed to the P–O bending vibration. The band at 1028 cm<sup>-1</sup> corresponds to the P–F stretching vibration.<sup>6</sup>

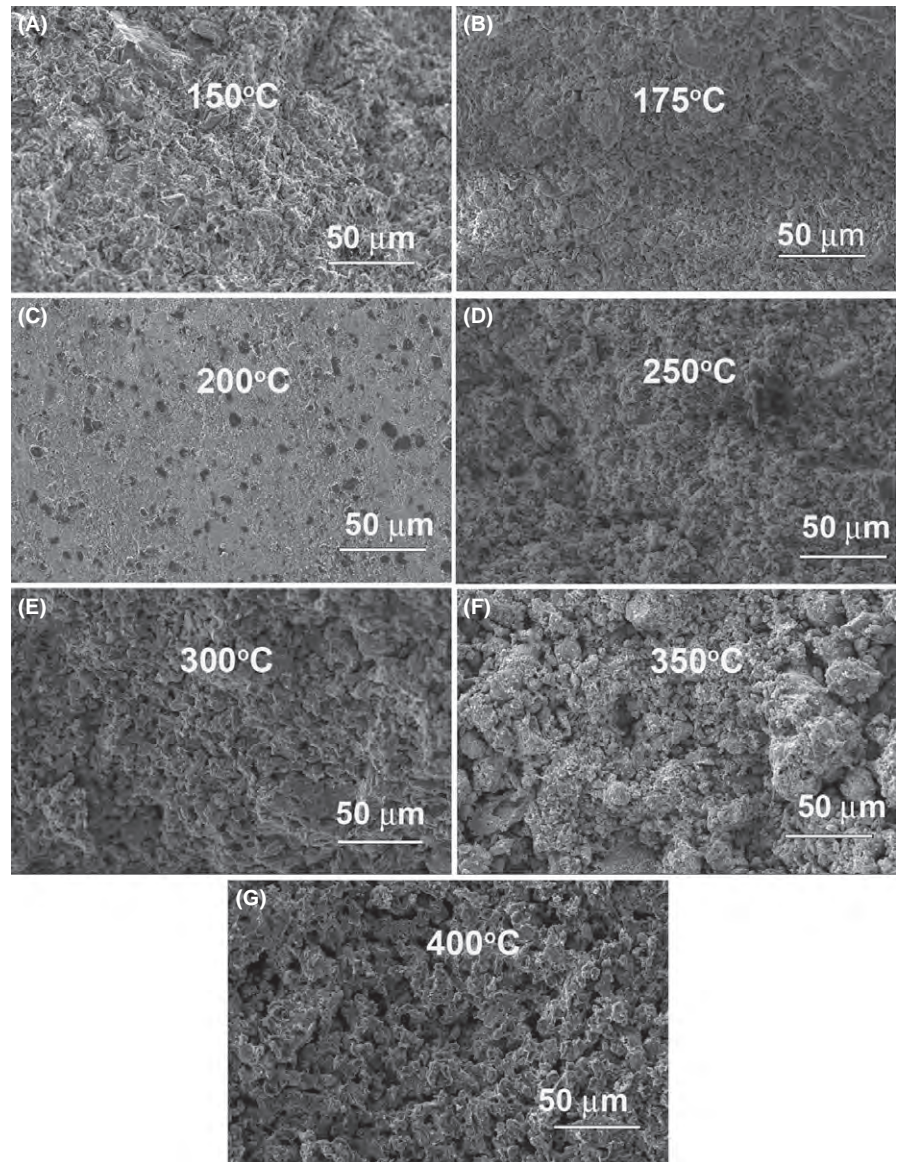
The glass-transition temperature of 45SnF<sub>2</sub>:25SnO:30P<sub>2</sub>O<sub>5</sub> glass as determined by the DSC is found to be about ~93°C (see Figure 2A). Liu et al. reported that the glass-transition temperature of 45SnF<sub>2</sub>:25SnO:30P<sub>2</sub>O<sub>5</sub> at about 135°C.<sup>6</sup> The difference in the  $T_g$  value in the present study as compared to the reported value may be due to the difference in melting time duration, origin and purity of chemicals, furnace heating conditions, and so on. The TG/DTA of SSP glass is shown in Figure 2B. The exothermic peak in the DTA curve at 163°C is attributed to crystallization of SnF<sub>2</sub> and SnO<sub>2</sub> formed by the oxidation of SnO<sub>2</sub> and the endothermic peak at ~343°C in the DTA curve corresponds to the onset of the melting of the individual components in the glass, particularly SnF<sub>2</sub> as evident from XRD (Figure 5). The weight loss found in the TG curve can be attributed to the volatilization loss of fluorine and hydroxyl by forming hydrogen Fluoride during melting.<sup>6</sup>

Table 1 gives the dielectric properties of SSP glass. In general, the density of the glasses depends on the atomic weight of the individual components used in the glass as



**FIGURE 4** XRD pattern of Al<sub>2</sub>O<sub>3</sub>-SSP glass composite sintered at different temperatures (150°C–400°C)





**FIGURE 5** Microstructure of fractured surfaces of  $\text{Al}_2\text{O}_3$ -SSP glass composite sintered at (A) 150°C, (B) 175°C, (C) 200°C, (D) 250°C, (E) 300°C, (F) 350°C, and (G) 400°C

well as the compactness of the structure units in the glass.<sup>29</sup> The density of the SSP glass is obtained as  $4.38 \text{ g cm}^{-3}$ . For most of the glasses, the dielectric constant depends on ionic and electronic polarization, while the dielectric loss depends on relaxations.<sup>4</sup> Dielectric loss in the glass is mainly due to conductance, ion relaxation, deformation, and vibration.<sup>11</sup> At low frequencies, ion relaxation and conductance losses are predominant.<sup>5</sup> The dielectric constant and dielectric loss at 1 MHz are 20 and 0.02, respectively. The dielectric constant for  $45\text{SnF}_2:25\text{SnO}:30\text{P}_2\text{O}_5$  glass at microwave frequency is found to be 16 (6.2 GHz). The quality factor ( $Q_u \times f$ ) is obtained as 990 GHz. The  $\epsilon_r$  value for the thin sheet of  $45\text{SnF}_2:25\text{SnO}:30\text{P}_2\text{O}_5$  glass measured at 5 GHz is 17 with  $\tan\delta$  0.006. The small variation in  $\epsilon_r$  of SSP glass in two methods (Hakki and split post dielectric resonator [SPDR]) is due to the difference in frequency used for measurement and the use of thin sheet and large bulk samples with slight

variations in density. The density reported for the bulk SSP glass in the present study is  $4.38 \text{ g cm}^{-3}$ . However, the sample used for SPDR measurement is very thin compared to the bulk and has a lower density of  $4.30 \text{ g cm}^{-3}$ . The difference in density of the samples used for determining the dielectric constant using Hakki and SPDR method is the possible reason for the difference in dielectric constant. In the microwave frequency region, only ionic and electronic polarization contributes to dielectric constant.<sup>12</sup> For practical applications, the resonant frequency should be independent of temperature variations.  $\tau_f$  value of SSP glass is found to be  $-290 \text{ ppm/}^\circ\text{C}$  measured in the temperature range 25°C–60°C.

The knowledge about thermal expansion studies of the SSP glass is very crucial for practical applications. Figure 3 shows the linear expansion of SSP glass in the temperature range 30°C–100°C. The CTE value for the  $45\text{SnF}_2:25\text{SnO}:30\text{P}_2\text{O}_5$  is found to be  $17.8 \text{ ppm/}^\circ\text{C}$  which is very close to

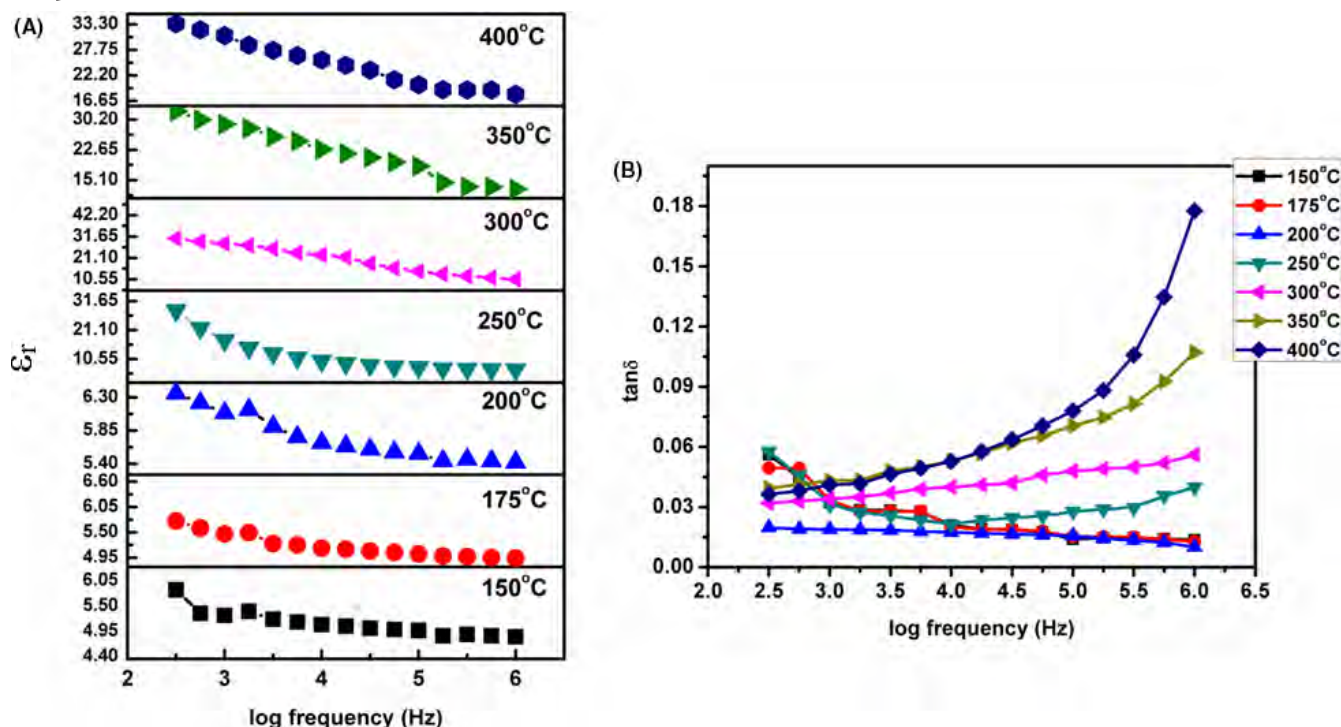


**FIGURE 6** Variation in (A) dielectric constant and (B) dielectric loss with radiofrequency for Al<sub>2</sub>O<sub>3</sub>-SSP glass composites sintered at different temperatures (150°C-400°C)

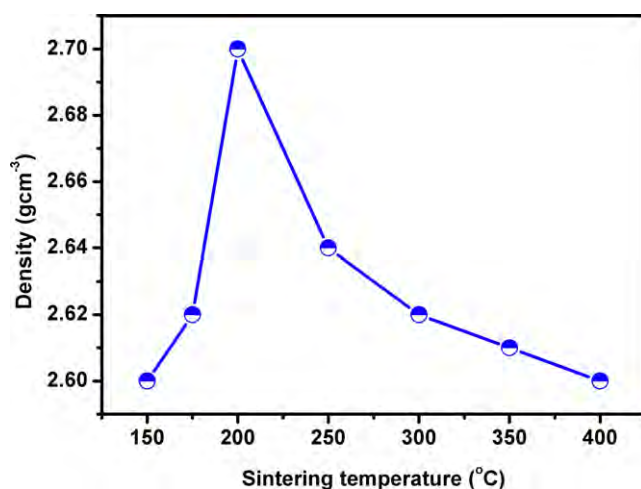


**FIGURE 7** Variation in density with sintering temperature for Al<sub>2</sub>O<sub>3</sub>-SSP glass

that reported by Liu et al. The photograph of SSP glass is shown in the inset of Figure 3. It has been reported that low  $T_g$  glasses would have higher CTE value.<sup>6</sup> The  $T_g$  value obtained for the SSP glass from CTE measurement is about ~95°C and is in agreement with that obtained from DSC analysis (Figure 2A).

### 3.2 | Structural, dielectric, and thermal properties of Al<sub>2</sub>O<sub>3</sub>-SSP glass composite

The XRD patterns of the Al<sub>2</sub>O<sub>3</sub>-SSP glass composite sintered at different temperatures (150°C-400°C) are shown in Figure 4. It is found that SSP glass which has a low  $T_g$  glass, recrystallizes to form the individual components of the glass and react to form secondary phases at higher temperatures. The XRD pattern shows the peaks of Al<sub>2</sub>O<sub>3</sub> (JCPDS file no. 88-0107), SnO<sub>2</sub> (JCPDS file no. 88-0287), SnF<sub>2</sub> (JCPDS file no. 71-2018), and secondary phases of SnP<sub>2</sub>O<sub>7</sub> (JCPDS file no. 75-1143) and Sn<sub>3</sub>(PO<sub>4</sub>)<sub>2</sub> (JCPDS file no. 70-0391) are also identified. The DSC and TG/DTA analysis of the SSP glass indicates that crystallization starts at about 150°C. The glass in the composite crystallizes into SnO<sub>2</sub>, SnF<sub>2</sub> and is evident in the XRD of the sample sintered at 150°C. Above 200°C, the SnF<sub>2</sub> melts and peaks become very weak indicating that fluorine is escaping. The SnO<sub>2</sub> reacts with P<sub>2</sub>O<sub>5</sub> to form SnP<sub>2</sub>O<sub>7</sub> and Sn<sub>3</sub>(PO<sub>4</sub>)<sub>2</sub> and is supported by the DSC and TG/DTA curves.

Figure 5 shows the microstructure of the fractured surface of Al<sub>2</sub>O<sub>3</sub>-SSP glass composite in the temperature range 150°C-400°C. The SEM pictures show the presence of secondary phases. Al<sub>2</sub>O<sub>3</sub> do not react with SSP glass in the entire sintering temperature range. The porosity of the composite increases above 200°C due to escape of



fluorine. The deficiency of fluorine lead to the crystallization of  $\text{SnP}_2\text{O}_7$  and  $\text{Sn}_3(\text{PO}_4)_2$  at temperatures above  $200^\circ\text{C}$ .

Figure 6 shows the variation in dielectric properties of the  $\text{Al}_2\text{O}_3$ -SSP glass composite measured in the radiofrequency region for the samples sintered at different temperature range  $150^\circ\text{C}$ - $400^\circ\text{C}$ . The dielectric constant is found to increase with increase in sintering temperature and is attributed to the formation of secondary phases. The increased amount of secondary phase formation and phase transition of tin-based phosphates may be the possible reason for the increase in dielectric constant at higher temperatures. The formation of secondary phases during sintering at different temperatures and vaporization of fluorine may be responsible for the variations in dielectric properties. The contribution of extrinsic loss is more predominant in  $\text{Al}_2\text{O}_3$ -SSP glass composite. Impurities, microstructural defects, grain boundaries, porosity, and so on, in the composite lead to high dielectric losses.<sup>3,15,30</sup> It has been reported that  $\text{SnP}_2\text{O}_7$  undergoes phase transitions at  $287^\circ\text{C}$  and  $557^\circ\text{C}$ <sup>31</sup> which may affect the dielectric properties. The composite sintered at  $200^\circ\text{C}$  has  $\epsilon_r=5.41$  with a  $\tan\delta$  of 0.01 at 1 MHz. The composite sintered above  $200^\circ\text{C}$ , show an increase in dielectric loss with frequency due to the increased amount of porosity in the composite. At  $200^\circ\text{C}$  temperature, the dielectric properties of the composite are found to be good for ULTCC practical applications. The dielectric properties of the composite can be tailored according to the need by sintering at different temperatures. Figure 7 shows the variation of density with sintering temperature for  $\text{Al}_2\text{O}_3$ -SSP glass composite. The density of the composites drops after  $200^\circ\text{C}$  which in turn increases the porosity in the composite. The decrease in density after  $200^\circ\text{C}$  also supports the escape of fluorine from  $\text{Al}_2\text{O}_3$ -SSP composite. The dielectric properties of the secondary

phase's particularly tin phosphates are not known due to the difficulty in getting sintered pellets of these materials. Hibino et al. also observed the same difficulty in sintering  $\text{SnP}_2\text{O}_7$  ceramic.<sup>32</sup> The precise knowledge about the dielectric properties of these secondary phases are needed to account for the anomalous trend observed in dielectric properties over the range of sintering temperature.

Figure 8 shows the variation of  $\epsilon_r$ ,  $Q_u \times f$ , and  $\tau_f$  for  $\text{Al}_2\text{O}_3$ -SSP glass composite as a function of sintering temperature at microwave frequency. In the microwave frequency, the dielectric constant varies between 4.6 and 17.0. The composite sintered at  $200^\circ\text{C}$  has dielectric constant of 5.20 (11 GHz). The microwave dielectric properties of the  $\text{Al}_2\text{O}_3$ -SSP glass composite revealed that with increase in sintering temperature, the  $Q_u \times f$  values increases up to  $350^\circ\text{C}$  and further increase in sintering temperature decreases the quality factor. However, the dielectric

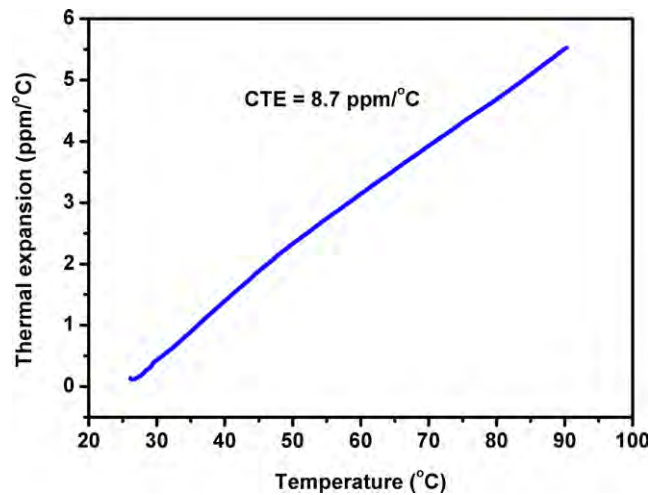


FIGURE 9 Thermal expansion study of  $\text{Al}_2\text{O}_3$ -SSP glass composite sintered at  $200^\circ\text{C}$

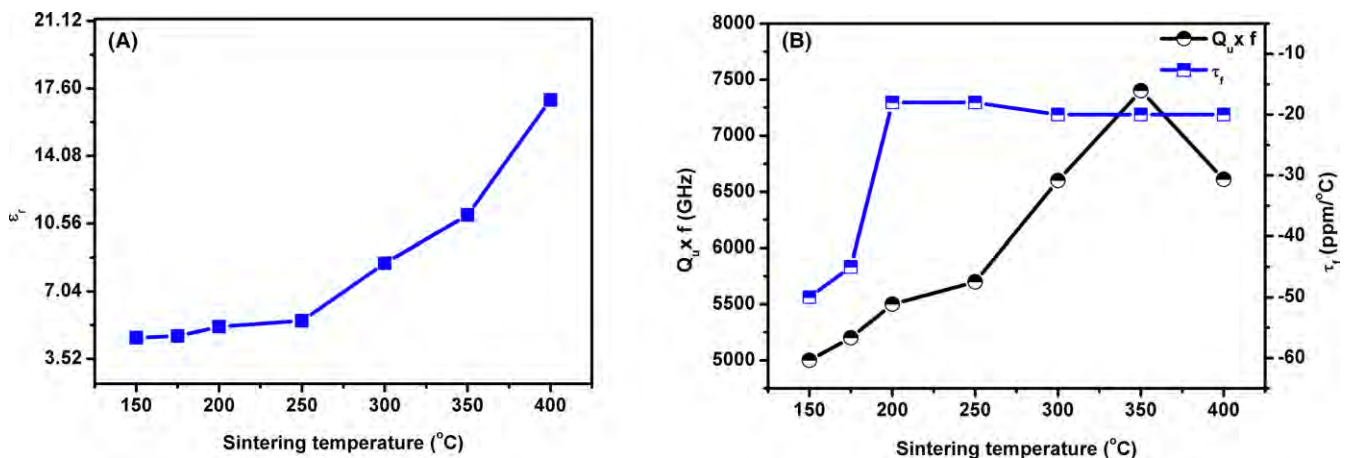


FIGURE 8 Variation in (A)  $\epsilon_r$ , (B)  $Q_u \times f$ , and  $\tau_f$  for  $\text{Al}_2\text{O}_3$ -SSP glass composite at microwave frequency with sintering temperature ( $150^\circ\text{C}$ - $400^\circ\text{C}$ )

constant increases with increase in sintering temperature. It may be noted that the secondary phases are formed in the composite at different sintering temperatures. The  $\tau_f$  value is small for the samples sintered at 200°C and 250°C. In the present study, the  $\text{Al}_2\text{O}_3$ -SSP glass composite sintered at 200°C (2 h) has  $Q_u \times f$  value 5500 GHz with  $\tau_f$  of  $-18$  ppm/°C. The possible error in the measurement of  $\epsilon_r$  using Hakki-Coleman method is of the order of 0.3%.<sup>30</sup> The increased glass content, secondary phase formation, and poor densification of the samples may be the reason for the relatively low quality factor. However, the material has a very low sintering temperature.

The thermal expansion studies of the  $\text{Al}_2\text{O}_3$ -SSP glass composite is carried out in the temperature range 30°C-90°C and the linear dimensional change with temperature is shown as Figure 9. The bulk composite sintered at 200°C has a CTE value of 8.7 ppm/°C. The thermal conductivity of the composite is very important for electronic applications. The room-temperature thermal conductivity of the  $\text{Al}_2\text{O}_3$ -SSP glass composite is 0.47 W/m/K. It has been reported that phosphate glasses have low thermal conductivity as well as higher thermal expansion as compared to the silicate glasses.<sup>29</sup>

## 4 | CONCLUSIONS

A novel composition based on  $\text{Al}_2\text{O}_3$ -SSP glass has been developed for ULTCC applications. The  $45\text{SnF}_2:25\text{SnO}:30\text{P}_2\text{O}_5$  glass has good dielectric properties both in radio ( $\epsilon_r$  of 20 and  $\tan\delta$  of 0.007 at 1 MHz) and microwave frequencies ( $\epsilon_r$  of 16 [6.2 GHz],  $Q_u \times f=990$  GHz with a  $\tau_f$  value of  $-290$  ppm/°C). The CTE value of  $45\text{SnF}_2:25\text{SnO}:30\text{P}_2\text{O}_5$  glass is found to be 17.8 ppm/°C. The  $\text{Al}_2\text{O}_3$ -SSP glass composite sintered below 200°C indicates the presence of  $\text{Al}_2\text{O}_3$ ,  $\text{SnF}_2$  and  $\text{SnO}_2$  and above 200°C,  $\text{SnP}_2\text{O}_7$ ,  $\text{Sn}_3(\text{PO}_4)_2$  are identified from the XRD. The  $\text{Al}_2\text{O}_3$ -SSP glass composite sintered at 200°C (2 h) has  $\epsilon_r=5.41$  with a  $\tan\delta$  of 0.01 at 1 MHz and  $\epsilon_r=5.20$  (11 GHz) with  $Q_u \times f=5500$  GHz with temperature coefficient of resonant frequency ( $\tau_f$ )= $-18$  ppm/°C at microwave frequency. The room-temperature thermal conductivity of the  $\text{Al}_2\text{O}_3$ -SSP glass composite is 0.47 W/m/K and CTE in the temperature range 30°C-90°C is found to be 8.7 ppm/°C.

## ACKNOWLEDGMENTS

I. J. Induja is grateful to Kerala State Council for Science Technology and Environment (KSCSTE), Kerala, India for providing the research fellowship. The authors thank Dr. K. P. Surendran for the constant support; Dr. P. Prabhakar Rao, Mr. Prithviraj, and Mrs. Soumya for recording XRD and SEM facilities; Dr. E. Bhoje Gowd for DSC measurement; and Dr. T. P. D Rajan for TG/DTA measurements.

## REFERENCES

1. Aziz DAA, Ahmed SE. Densification and dielectric properties of  $\text{SrO-Al}_2\text{O}_3\text{-B}_2\text{O}_3$  ceramic bodies. *Bull Mater Sci*. 2011;34(1):143-148.
2. Sebastian MT, Wang H, Jantunen H. Low temperature co-fired ceramics with ultra-low sintering temperature: a review. *Curr Opin Solid State Mater Sci*. 2016;20(3):151-170.
3. Sebastian MT, Jantunen H. Low loss dielectric materials for LTCC applications: a review. *Int Mater Rev*. 2008;53(2):57-90.
4. Yu H, Liu J, Zhang W, Zhang S. Ultra-low sintering temperature ceramics for LTCC applications: a review. *J Mater Sci: Mater Electron*. 2015;26(12):9414-9423.
5. Sebastian MT, Ulic R, Jantunen H. Low-loss dielectric ceramic materials and their properties. *Int Mater Rev*. 2015;60(7):392-412.
6. Liu H, Ma J, Gong J, Xu J. The structure and properties of  $\text{SnF}_2\text{-SnO-P}_2\text{O}_5$  glasses. *J Non-Cryst Solid*. 2015;419:92-96.
7. Masai H, Tanimoto T, Fujiwara T, et al. Fabrication of Sn-doped zinc phosphate glass using a platinum crucible. *J Non-Cryst Solid*. 2012;358(2):265-269.
8. Eht D. Fluoro aluminate glasses for lasers and amplifiers. *Curr Opin Solid State Mater Sci*. 2003;7(2):135-141.
9. Nardia RPRD, Braza CE, Pereira C, et al. Crystallization in lead tungsten fluorophosphate glasses. *J Mater Res*. 2015;18(1):228-232.
10. Yamane M, Asahara Y. *Glasses for Photonics*. United Kingdom: Cambridge University Press; 2004.
11. Stević S, Aleksić R, Backovi N. Influence of fluorine on thermal properties of fluorophosphate glasses. *J Am Ceram Soc*. 1987;70(10):264-265.
12. Trimble J, Golovchak R, Oelgoetz J, Brennan C, Kovalskiy A. Structural characterization of tin fluorophosphates glasses doped with  $\text{Er}_2\text{O}_3$ . *Phys Chem Glasses Eur J Glass Sci Technol B*. 2016;57:27-31.
13. Yu M, Zhang J, Li X, et al. Optimization of the tape casting process for development of high performance alumina ceramics. *Ceram Int*. 2015;41(10):14845-14853.
14. Ibrahim A, Alias R, Ambak Z, et al. In characterization of alumina-based LTCC composite materials: thermal and electrical properties. In *Proceedings of the 12th Electronics Packaging Technology Conference*, 2010:269-272.
15. Alford NM, Penn SJ. Sintered alumina with low dielectric loss. *J Appl Phys*. 1996;80(10):5895-5898.
16. Chen X, Zhang W, Bai S, Du Y. Densification and characterization of  $\text{SiO}_2\text{-B}_2\text{O}_3\text{-CaO-MgO}$  glass/ $\text{Al}_2\text{O}_3$  composites for LTCC application. *Ceram Int*. 2013;39(6):6355-6361.
17. Yoon S, Kim K, Kim S, Shim S, Park J. Densification and dielectric properties of glass/ceramic composites sintered with various borosilicate. *Glass Mater Sci Forum*. 2007;544-545:961-964.
18. Chiang CC, Wang S, Wang YR, Cheng W, Wei J. Densification and microwave dielectric properties of  $\text{CaO-B}_2\text{O}_3\text{-SiO}_2$  system glass-ceramics. *Ceram Int*. 2008;34(3):599-604.
19. Hsiang HI, Mei LT, Yang SW, Liao WC, Yen FS. Effect of alumina on the crystallization behavior, densification and dielectric properties of  $\text{BaO-ZnO-SrO-CaO-Nd}_2\text{O}_3\text{-TiO}_2\text{-B}_2\text{O}_3\text{-SiO}_2$  glass-ceramics. *Ceram Int*. 2011;37(7):2453-2458.
20. Li E, Shi Y, Sun C, Zhao Y, Zhang S. Effect of  $\text{SrTiO}_3$  on the properties of CBS glasses/ $\text{Al}_2\text{O}_3$  ceramics. *J Mater Sci: Mater Electron*. 2016;27(6):6592-6597.



21. Yoon S, Shim S, Kim K, Park J, Kim S. Low temperature preparation and microwave dielectric properties of ZBS glass-Al<sub>2</sub>O<sub>3</sub> composites. *Ceram Int.* 2009;35(3):1271-1275.
22. Rajesh S, Jantunen H, Letz M, Willhelm S. Low temperature sintering and dielectric properties of alumina-filled glass composites for LTCC applications. *Int J Appl Ceram Technol.* 2011;9(1):52-59.
23. Ming L, Hongqing Z, Haikui Z, Zehnxing Y, Jianxin Z. Low temperature sintering and dielectric properties of Ca-Ba-Al-B-Si-O glass/Al<sub>2</sub>O<sub>3</sub> composites for LTCC applications. *J Wuhan University of Technology, Mater Sci.* 2013;28(6):1085-1090.
24. Induja IJ, Abhilash P, Arun S, Surendran KP, Sebastian MT. LTCC tapes based on Al<sub>2</sub>O<sub>3</sub>-BBSZ glass with improved thermal conductivity. *Ceram Int.* 2015;41(10):13572-13581.
25. Luo X, Ren L, Xie W, et al. Microstructure, sintering and properties of CaO-Al<sub>2</sub>O<sub>3</sub>-B<sub>2</sub>O<sub>3</sub>-SiO<sub>2</sub> glass/Al<sub>2</sub>O<sub>3</sub> composites with different CaO contents. *J Mater Sci: Mater Electron.* 2016;27(5):5446-5545.
26. Kim K, Shim S, Kim S, Yoon S. Sintering behavior and dielectric properties of ceramic/glass composites using lead borosilicate glass. *J Ceram Process Res.* 2010;11(1):35-39.
27. Ignatieva LN, Surovtsev NV, Plotnichenko VG, et al. The peculiarities of fluoride glass structure. Spectroscopic study. *J Non-Cryst Solid.* 2007;353(13-15):1238-1242.
28. Winegar JY, Harper JT, Brennan C, Oelgoetz J, Kovalskiy A. Structure of SnF<sub>2</sub>-SnO-P<sub>2</sub>O<sub>5</sub> glasses. *Phys Procedia.* 2013;44:159-165.
29. Li Y, Yang J, Xu S, Wang G, Hu L. Physical and thermal properties of P<sub>2</sub>O<sub>5</sub>-Al<sub>2</sub>O<sub>3</sub>-BaO-La<sub>2</sub>O<sub>3</sub> glass. *J Mater Sci Technol.* 2005;21(3):391-394.
30. Sebastian MT. *Dielectric Materials for Wireless Communication.* Oxford: Elsevier; 2008.
31. Gover RKB, Withers ND, Allen S, Wither RL, Evans JSO. Structure and phase transitions of SnP<sub>2</sub>O<sub>7</sub>. *J Solid State Chem.* 2002;166(1):42-48.
32. Shen Y, Nishida M, Kanematsu W, Hibino H. Synthesis and characterization of dense SnP<sub>2</sub>O<sub>7</sub>-SnO<sub>2</sub> composite ceramics as intermediate-temperature proton conductors. *J Mater Chem.* 2011;21:663-670.

**How to cite this article:** Induja IJ, Sebastian MT. Microwave dielectric properties of SnO-SnF<sub>2</sub>-P<sub>2</sub>O<sub>5</sub> glass and its composite with alumina for ULTCC applications. *J Am Ceram Soc.* 2017;00:1-9.